

Observations at arcsecond resolution of steep-spectrum sources which vary at low frequencies

F. Mantovani,¹ W. Junor,^{1,2} R. Fanti,^{1,3} L. Padrielli,¹ I. W. A. Browne⁴ and T. W. B. Muxlow⁴

¹ *Istituto di Radioastronomia del CNR, Via Irnerio 46, I-40126 Bologna, Italy*

² *National Radio Astronomy Observatory, PO Box 0, Socorro, NM 87801–0387, USA*

³ *Dipartimento di Fisica, Università degli Studi, Via Irnerio 46, I-40126, Bologna, Italy*

⁴ *Nuffield Radio Astronomy Laboratories, Jodrell Bank, Macclesfield, Cheshire SK11 9DL*

Accepted 1992 February 2. Received 1992 January 31; in original form 1991 December 12

SUMMARY

We present VLA 5-GHz and MERLIN 408-MHz observations of a sample of steep-spectrum low-frequency-variable sources. The radio observations show that the vast majority of sources have linear sizes typical of the compact steep spectrum sources. A classification based on their arcsecond-scale structure allows us to separate them into two classes, namely sources with an unresolved component and lobe-dominated sources. All but three sources show the existence of compact (subarcsecond) components which are required by models which explain the source variability as due to propagation effects in the interstellar medium. There are indications that the hotspots are the origin of the variability in lobe-dominated sources.

Key words: radiative transfer – interstellar medium: general – radio continuum: galaxies.

1 INTRODUCTION

Propagation effects through the interstellar medium are now believed to be responsible for the low-frequency variability (LFV) commonly observed among flat-spectrum radio sources (Shapirovskaia 1982; Rickett, Coles & Bourgois 1984; Gregorini, Ficarra & Padrielli 1986; Spangler *et al.* 1989; Mantovani *et al.* 1990a). Intrinsic mechanisms (Rees 1966; Jones & Burbidge 1973; Burbidge, Jones & O'Dell 1974; Blandford & Königl 1979) are responsible for the observed variability in a minority of cases (10–15 per cent). In such processes the LFV is the relic of outbursts occurring first at higher frequencies and shifting to lower frequencies with time (Dennison *et al.* 1984; Padrielli *et al.* 1987). Thus, for sources found to have variability over a broad frequency range, it is quite likely that both processes are at work at the same time.

In samples of steep-spectrum sources, only a small fraction of sources exhibit evidence of LFV. Moreover, they do not show variability at high frequency (Padrielli *et al.* 1987). This indicates that for these sources the variability is due to an extrinsic mechanism, making these sources suitable for observational tests of refractive scintillation (Rickett 1986). Furthermore we would expect that, by selecting steep-spectrum low-frequency-variable sources, we would pick out objects belonging to the class of compact steep-spectrum

(CSS) sources. This class of objects has been extensively investigated by several authors (e.g. van Breugel, Miley & Heckman 1984; Saikia 1988; Spencer *et al.* 1989; Fanti *et al.* 1990).

We have selected a sample of 19 sources with evidence of LFV ($\nu < 1$ GHz), and with an overall steep spectral index ($\alpha > 0.5$, $S \propto \nu^{-\alpha}$), from the papers of Cotton (1976), McAdam (1980 and private communication), Spangler & Cotton (1981), Fanti *et al.* (1983) and Altschuler *et al.* (1984). A preliminary stage of our investigation was to observe the selected sources at both arcsecond and milliarcsecond (mas) resolution, with the aim of:

- (i) mapping the sources in order to detect the high-brightness components required by the refractive scintillation theory and to measure their flux densities and sizes;
- (ii) deriving further information on the characteristics of the interstellar medium, and
- (iii) finding new CSS sources.

Five of the 19 sources of the sample had been observed already at both milliarcsecond and arcsecond resolution (see Section 3.3). We present here observations of the remainder made with the VLA A-configuration at 5 GHz (11 sources) and with MERLIN at 408 MHz (all the sources with Dec. $> -15^\circ$ except 1203+043). The VLBI observations and a discussion of the results will be given elsewhere.

2 VLA AND MERLIN OBSERVATIONS

The sources were observed with the VLA (Thompson *et al.* 1980, in the A-configuration on 1986 May 30 at 5 GHz (resolution ~ 0.4 arcsec) for periods of 10- to 20-min duration. Two intermediate-frequency (IF) channels separated by 50 MHz, each of 50-MHz bandwidth, were used. The data were calibrated in the usual way with standard AIPS tasks and then processed with the NRAO AIPS programs. The output of the two independent IFs were separately analysed, self-calibrated and then combined to produce the final image of the radio source.

The MERLIN (Thomasson 1986) 408-MHz observing dates are summarized in Table 1. The calibration source was 3C119 with an adopted flux density of 17.3 Jy. The data were calibrated and processed using both the Jodrell Bank OLAF package and the NRAO AIPS package. It is worth noting here that absolute positional information is lost for MERLIN maps.

3 RESULTS

3.1 Description of the maps and notes on individual sources

0114–211

This source was monitored at 408 MHz by McAdam (1980) and reported as ‘probably variable’. There are indications that it does not change in flux density at 1415 MHz (Giacani & Colomb 1988). This is common behaviour for sources in

our sample. We find two compact components separated by less than 1 arcsec in PA 90° (see Fig. 1). The optical counterpart is a weak galaxy (Morganti, private communication).

0235–197

Classified as a probably variable source at 408 MHz by McAdam (1980), this has the largest angular size (43 arcsec) in our sample. The VLA map (Fig. 2) shows the classical double structure of powerful radio galaxies. The optical counterpart is a faint galaxy (Prestage & Peacock 1983) with redshift 0.62 (Morganti, private communication).

Table 1. MERLIN observing date.

Source:	Other Name:	Obs.Date
0320 + 053	DA101	87 Sep 8
0358 + 004	3C99	84 Sep 27
0548 + 165	DA190	87 Sep 8
0725 + 147	3C181	87 May 5
0809 – 056		87 May 3
1239 – 044	3C275	87 Sep 8
1422 + 202	4C20.33	84 Mar 8
1524 – 136	OR-140	81 Jul 13
1741 + 279	4C27.28	87 May 5
2033 + 187		87 Sep 8
2147 + 145		87 Sep 8

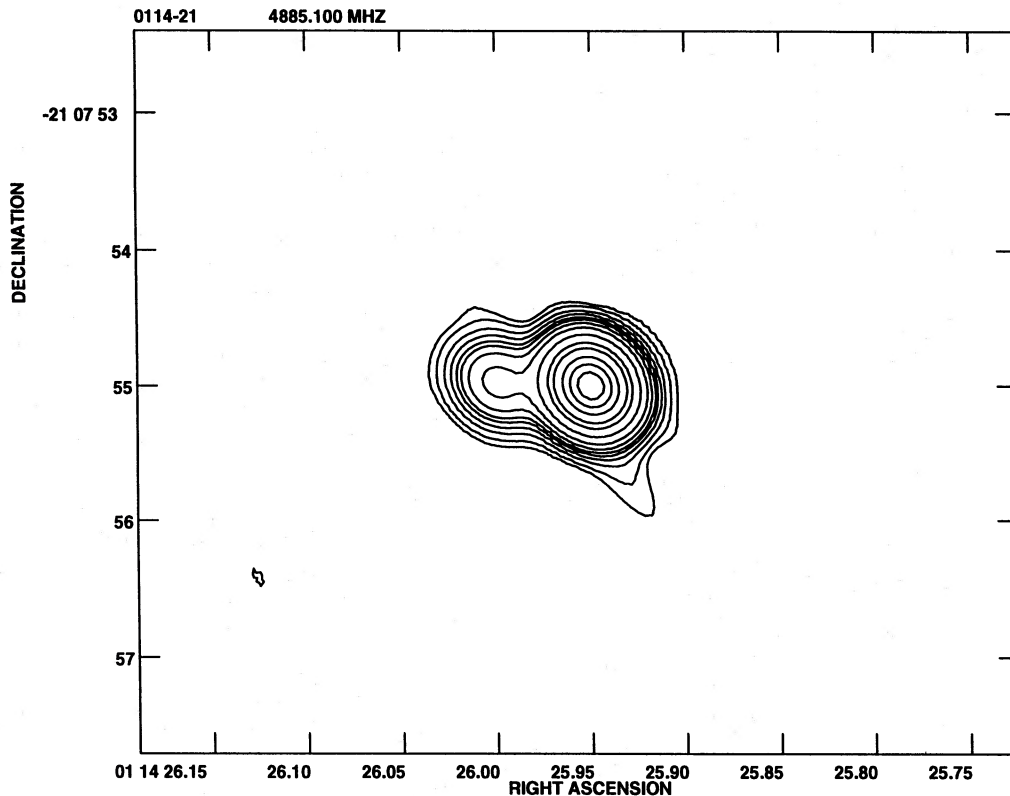


Figure 1. VLA map of 1114–211 at 4885 MHz with an angular resolution of 0.43×0.37 arcsec² along a PA of 36° . Peak brightness: 1071 mJy beam⁻¹. Contours: –1.5, 1.5, 3, 6, 10, 15, 20, 30, 50, 100, 200, 300, 500, 700 and 900 mJy beam⁻¹.

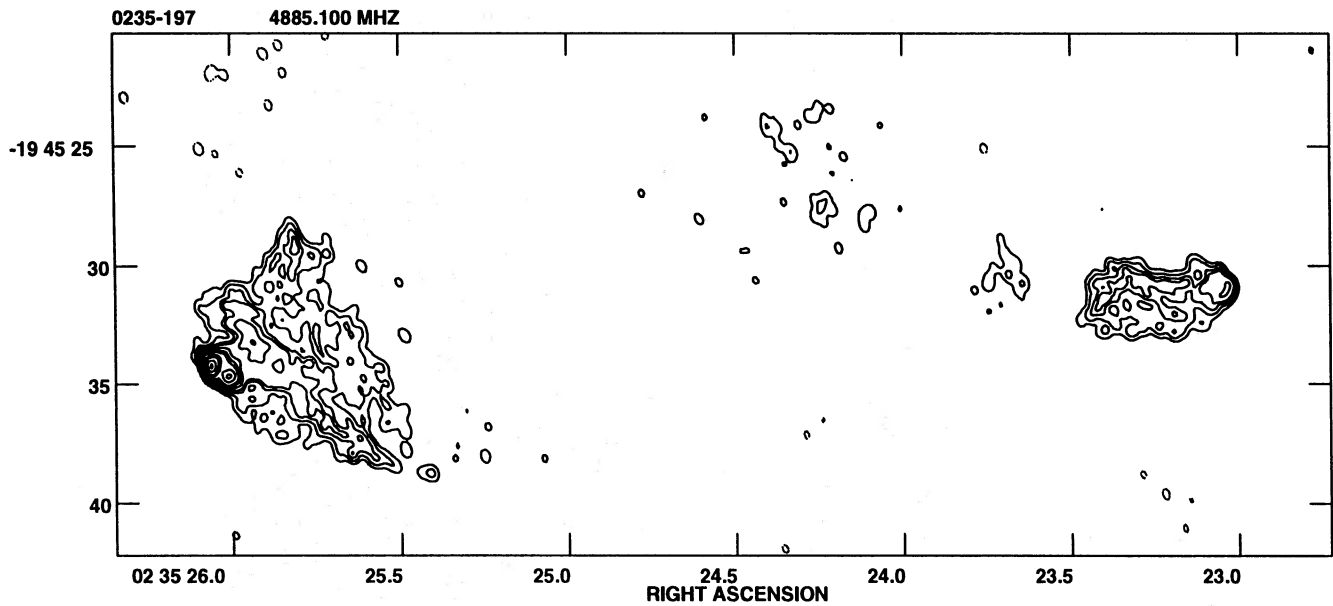


Figure 2. VLA map of 0235 – 197 at 4885 MHz with an angular resolution of 0.48×0.33 arcsec² along a PA of 22°. Peak brightness: 74 mJy beam⁻¹. Contours: -0.2, 0.2, 0.5, 1, 1.5, 3, 6, 10, 20, 30, 50, 70, 100, 150 and 200 mJy beam⁻¹.

0320 + 053

Fanti *et al.* (1983) listed this source as variable at 408 MHz. Multifrequency observations by Padrielli *et al.* (1987) show that it does not vary at frequencies between 4 and 15 GHz. The VLA map and the MERLIN map show a point-like source. Broderick & Condon (1985) reported a normalized fringe visibility of 0.55 in their VLBI observations at 430 MHz, corresponding to a Gaussian component of ~ 30 mas in angular size. They also found a faint galaxy as its optical counterpart.

0548 + 165 (DA190)

Fanti *et al.* (1983) listed this source as variable at 408 MHz. Douglas *et al.* (1980) defined it as ‘probably variable’ at 318 MHz. Multifrequency observations by Padrielli *et al.* (1987) show that 0548 + 165 does not vary at frequencies between 4 and 15 GHz. The VLA and MERLIN maps (Fig. 3a, b) show an asymmetric structure with a strong unresolved component coincident with a blue stellar object (BSO), and a much weaker secondary component about 3 arcsec away. The substructure in the northern component of the MERLIN map may be an artefact of the data processing. The source was also observed with VLBI at 430 MHz by Broderick & Condon (1975), who found a normalized fringe visibility of 0.51 corresponding to a Gaussian component of ~ 25 mas.

0725 + 147 (3C181)

This was reported as probably variable by McAdam (1980) at 408 MHz. Both our VLA and MERLIN maps (Fig. 4a, b) reveal a fairly symmetric double structure with a separation between the peaks of emission of about 6 arcsec. There is a bridge of emission joining the two lobes on the MERLIN map, while on the VLA map a weak core (9 mJy peak) is visible. The source is identified with a quasar of $m = 19$ and

$z = 1.382$ (Wills, Wills & Douglas 1973). It was also observed at 1.7 GHz with MERLIN by Cawthorne *et al.* (1986). Their map does not have the central feature detected by our VLA observations. They show that the percentage polarization distributions at 1.7 and 0.96 GHz are asymmetric, with the polarization confined to the south-east component.

0809 – 056

This is another source defined as probably variable by McAdam (1980). Its radio structure is that of a fairly symmetric double in both the VLA and MERLIN maps (Fig. 5a, b). In the VLA map no feature is seen between the two components above the detection limit (0.25 mJy beam⁻¹).

1203 + 043

This is the second largest source in our sample, having a major axis size of 30 arcsec. It was listed as probably variable by McAdam (1980). There is little information on this source available in the literature. Our 5-GHz VLA image (Fig. 6) shows an elongated, bent and blobby ‘jet’ on the southern side and a region of low-brightness emission on the opposite side of a fairly isolated compact component that may be the radio core of the source.

1239 – 045 (3C275)

McAdam (1980) listed this source as probably variable. The radio structure from both the VLA and MERLIN maps (Fig. 7a, b) is that of a double, rather symmetrical source. The two lobes have hotspots in their outer parts, as confirmed by a recent VLA 15-GHz map (Mantovani, in preparation). The north-east component has the higher percentage polarization (Davis, Stannard & Conway 1983). The optical counterpart is a galaxy of $m = 21$ and redshift 0.480 (Spinrad, Kron &

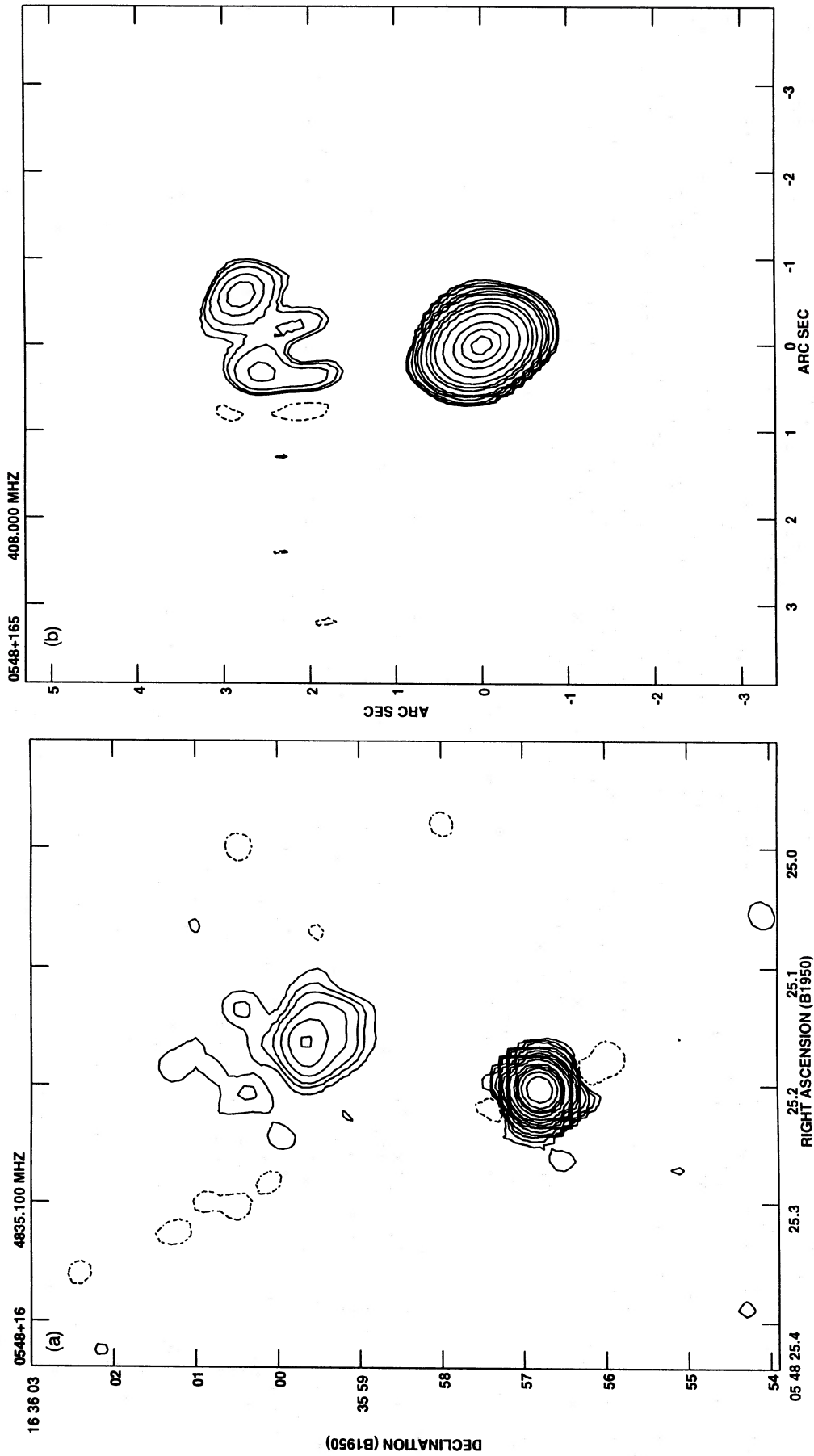


Figure 3. (a) VLA map of 0548 + 165 at 4835 MHz with an angular resolution of 0.35×0.34 arcsec² along a PA of -36° . Peak brightness: 892 mJy beam⁻¹. Contours: $-0.3, 0.3, 0.6, 1, 2, 4, 8, 12, 20, 30, 50, 100, 200, 300$ and 500 mJy beam⁻¹. (b) MERLIN map of 0548 + 165 at 408 MHz with an angular resolution of 0.6×0.5 arcsec² along a PA of 2.5° . Peak brightness: 4570 mJy beam⁻¹. Contours: $-15, 15, 20, 30, 50, 70, 100, 200, 300, 500, 1000, 2000, 3000, 4000$ and 5000 mJy beam⁻¹.

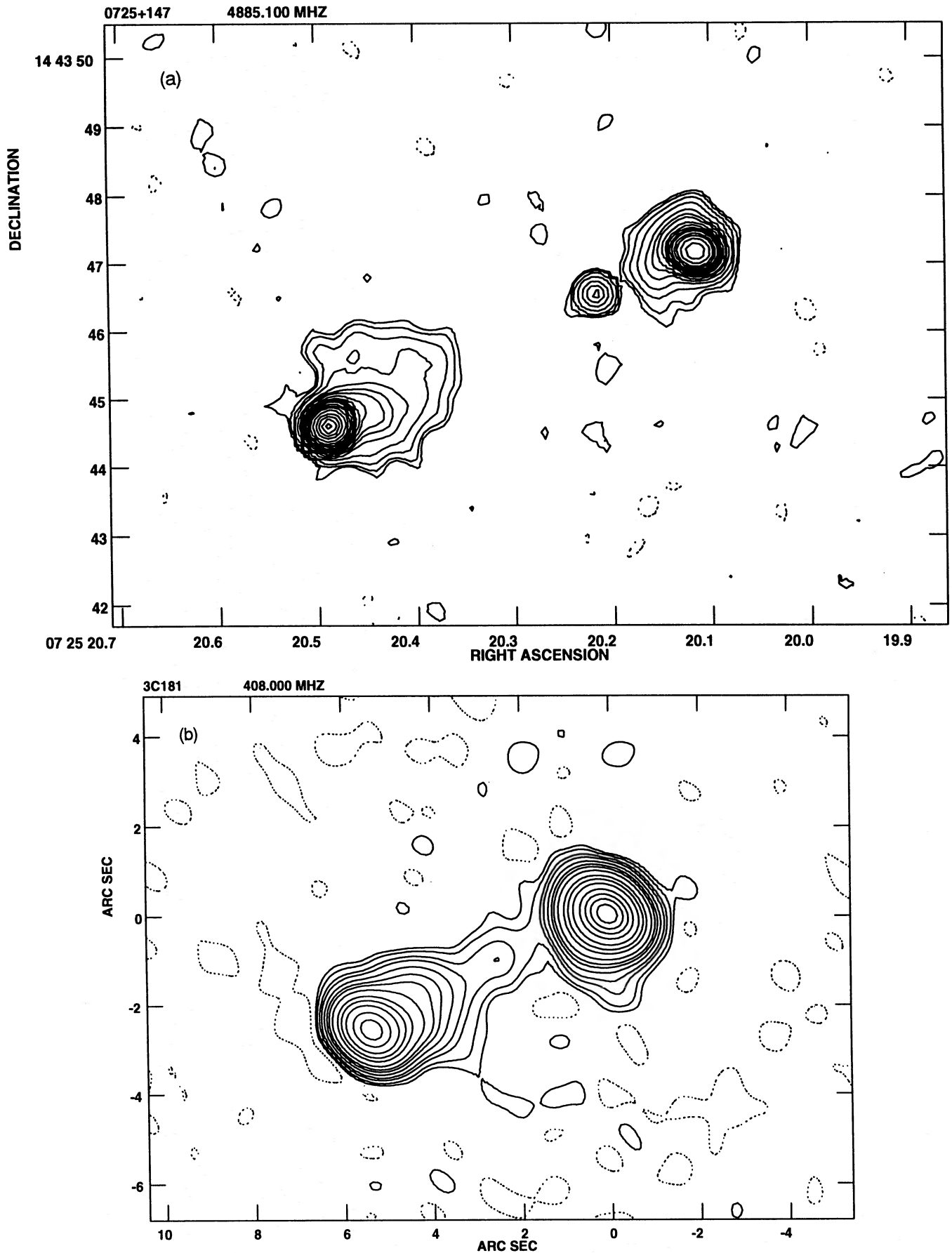


Figure 4. (a) VLA map of 0725 + 147 at 4885 MHz with an angular resolution of $0.34 \times 0.33 \text{ arcsec}^2$ along a PA of 87° . Peak brightness: $325 \text{ mJy beam}^{-1}$. Contours: $-0.3, 0.3, 0.5, 1, 2, 4, 6, 8, 12, 16, 20, 25, 30, 40, 50, 70, 100, 200, 250$ and $300 \text{ mJy beam}^{-1}$. (b) MERLIN map of 0725 + 147 at 408 MHz with an angular resolution of $1.1 \times 0.8 \text{ arcsec}^2$ along a PA of 55° . Peak brightness: $3361 \text{ mJy beam}^{-1}$. Contours: $-10, 10, 20, 40, 60, 100, 150, 200, 300, 500, 700, 1000, 1500, 2000, 2500$ and $3000 \text{ mJy beam}^{-1}$.

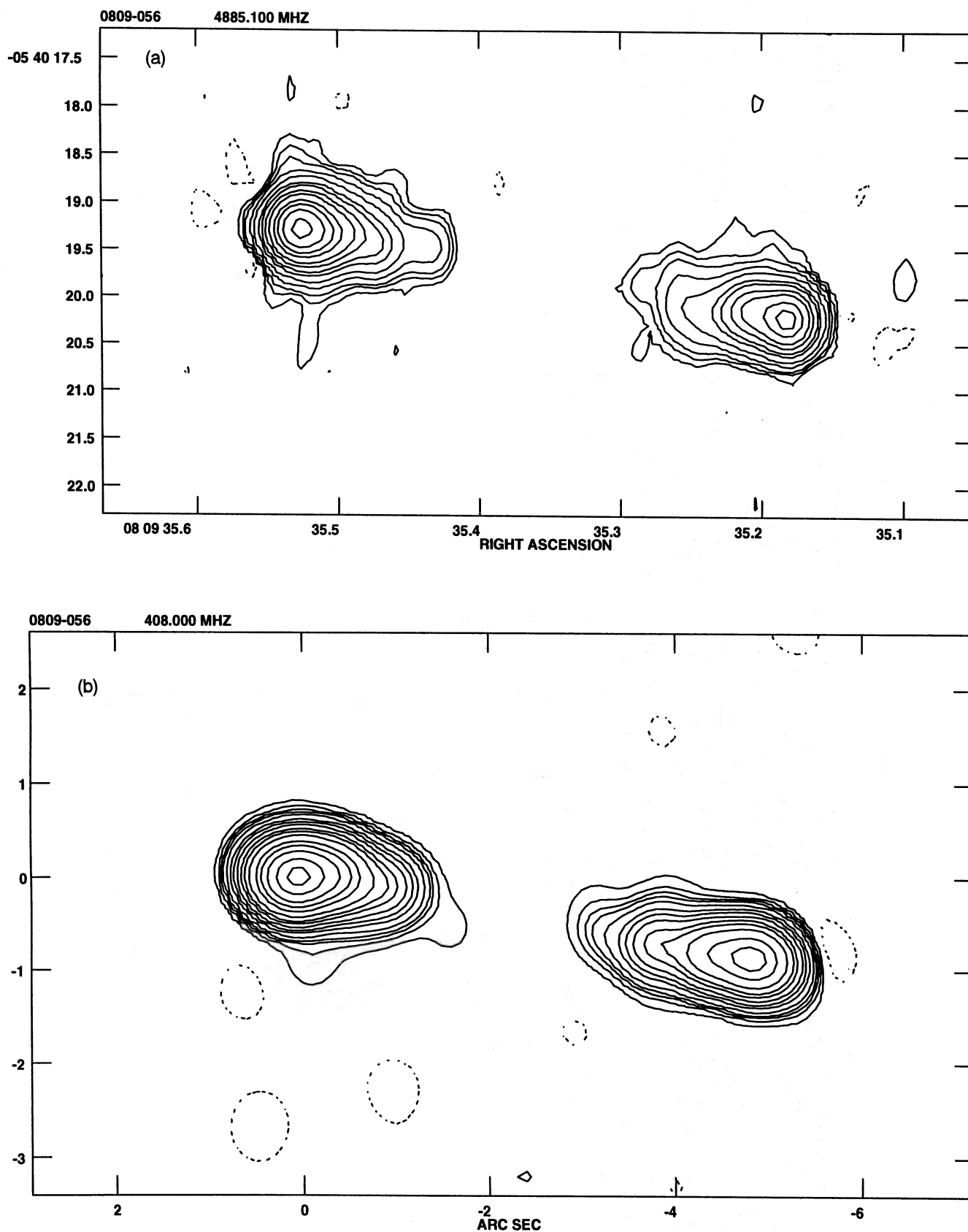


Figure 5. (a) VLA map of 0809–056 at 4885 MHz with an angular resolution of 0.42×0.35 arcsec² along a PA of -1° . Peak brightness: 176.8 mJy beam⁻¹. Contours: $-0.3, 0.3, 0.6, 1, 2, 4, 8, 12, 20, 30, 50, 70, 100, 150$ and 200 mJy beam⁻¹. (b) MERLIN map of 0809–056 at 408 MHz with an angular resolution of 0.5×0.5 arcsec². Peak brightness: 2206 mJy beam⁻¹. Contours: $-5, 5, 10, 15, 20, 30, 50, 70, 100, 150, 200, 300, 500, 700, 1000, 1500$ and 2000 mJy beam⁻¹.

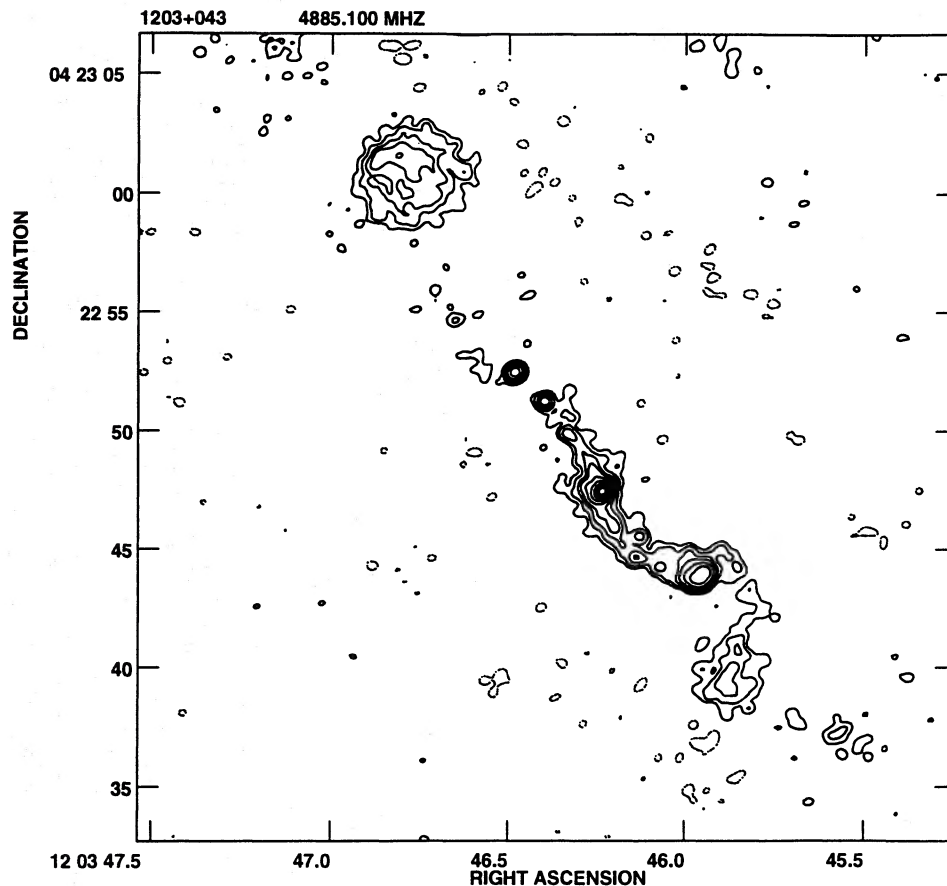


Figure 6. VLA map of 1203+043 at 4885 MHz with an angular resolution of 0.47×0.40 arcsec² along a PA of -67° . Peak brightness: 25 mJy beam⁻¹. Contours: $-0.15, 0.15, 0.3, 0.6, 1, 2, 4, 8, 12, 15, 20, 30, 50, 70, 100, 150, 200$ and 250 mJy beam⁻¹.

Hunstead 1979). This source was also observed with VLBI by Preston *et al.* (1985) at 2.29 GHz with a fringe spacing of about 3 mas. They found a correlated flux density <0.11 Jy and a fringe visibility of 0.049.

1245 – 197

McAdam (1980) listed this source as a definite variable at 408 MHz. Preston *et al.* (1985) reported a correlated flux density <0.06 Jy at 2.29 GHz and a fringe visibility <0.015 . It has been optically identified with a galaxy with a redshift of 1.275 (Morganti, private communication).

1422 + 202

Although reported as a variable source at 408 MHz by Fanti *et al.* (1983), there are no flux density variations with time at higher frequencies (Padielli *et al.* 1987). The VLA map (Fig. 8a) shows a structure elongated in the north–south direction, with a faint region off-axis close to the southern bright hot-spot. A similar structure is visible in the 408-MHz MERLIN map (Fig. 8b), where, however, part of the thin jet is not seen. The core of the source is the compact feature at the beginning of the jet in the VLA map, whose position coincides with that of a quasar of $m=17.6$ and $z=0.871$ (Argue, Kenworthy & Stewart 1973; Véron-Cetty & Véron 1987). This component has an inverted spectral index and is not detected in the MERLIN map. Preston *et al.* (1985) found a

correlated flux density <0.13 Jy at 2.29 GHz and a fringe visibility <0.111 . Bååth & Mantovani (1991) detected two milliarcsecond components about 8 arcsec apart from each other in PA 0° (EVN, MK3 Mode B observations at 1.7 GHz). The separation and position angle correspond to those of the core and the southern hotspot in the VLA map.

1524 – 136

This is the fastest varying source at 408 MHz found by Fanti *et al.* (1983). Multifrequency observations showed no change in flux density from 4.8 to 14.5 GHz (Padielli *et al.* 1987). The source is slightly resolved in both the VLA and the MERLIN maps. VLBI observations by Preston *et al.* (1985) gave a correlated flux <0.12 Jy and a fringe visibility <0.061 at 2.29 GHz. VLBI observations at 610 MHz (Mantovani, Muxlow & Padielli 1987) show that 1524 – 136 has an elongated structure in PA 45° . The overall size (400 mas) is comparable with that of the arcsecond-scale maps we have made. 1524 – 136 has been optically identified with a quasar with a redshift of 1.687 (Hunstead, private communication).

1741 + 279

This source was reported as variable at 408 MHz by Spangler & Cotton (1981). It was mapped only with MERLIN at 408 MHz (Fig. 9). Its structure is that of a triple source with a

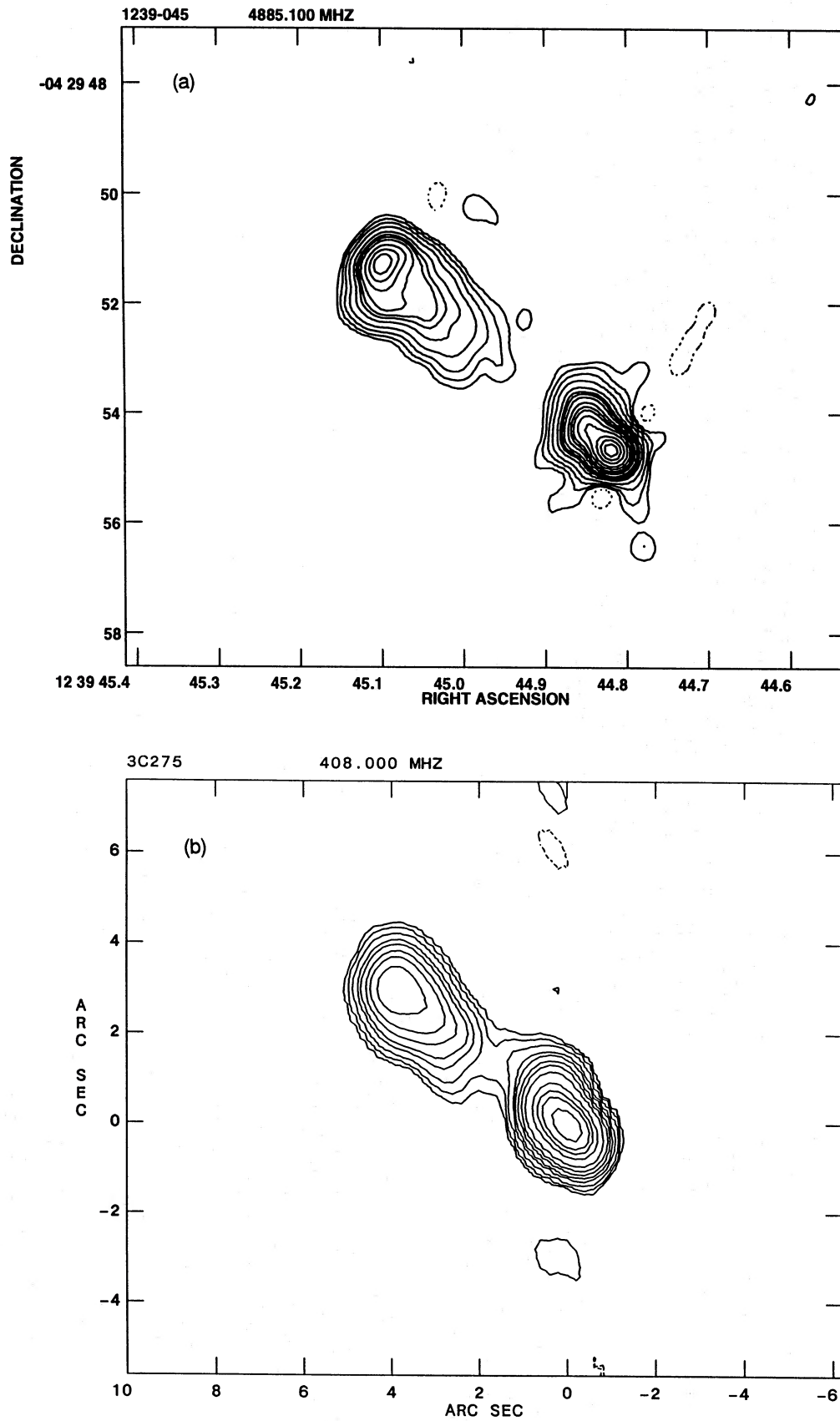


Figure 7. (a) VLA map of 1239–045 at 4885 MHz with an angular resolution of 0.43×0.38 arcsec² along a PA of -32° . Peak brightness: $294 \text{ mJy beam}^{-1}$. Contours: $-0.5, 0.5, 1, 2, 4, 8, 12, 15, 20, 30, 40, 50, 70, 100, 150, 200, 250$ and $300 \text{ mJy beam}^{-1}$. (b) MERLIN map of 1239–045 at 408 MHz with an angular resolution of 0.9×0.7 arcsec² along a PA of 22° . Peak brightness: $4097 \text{ mJy beam}^{-1}$. Contours: $-10, 10, 20, 40, 80, 120, 200, 300, 500, 1000, 1500, 2000, 3000$ and $5000 \text{ mJy beam}^{-1}$.

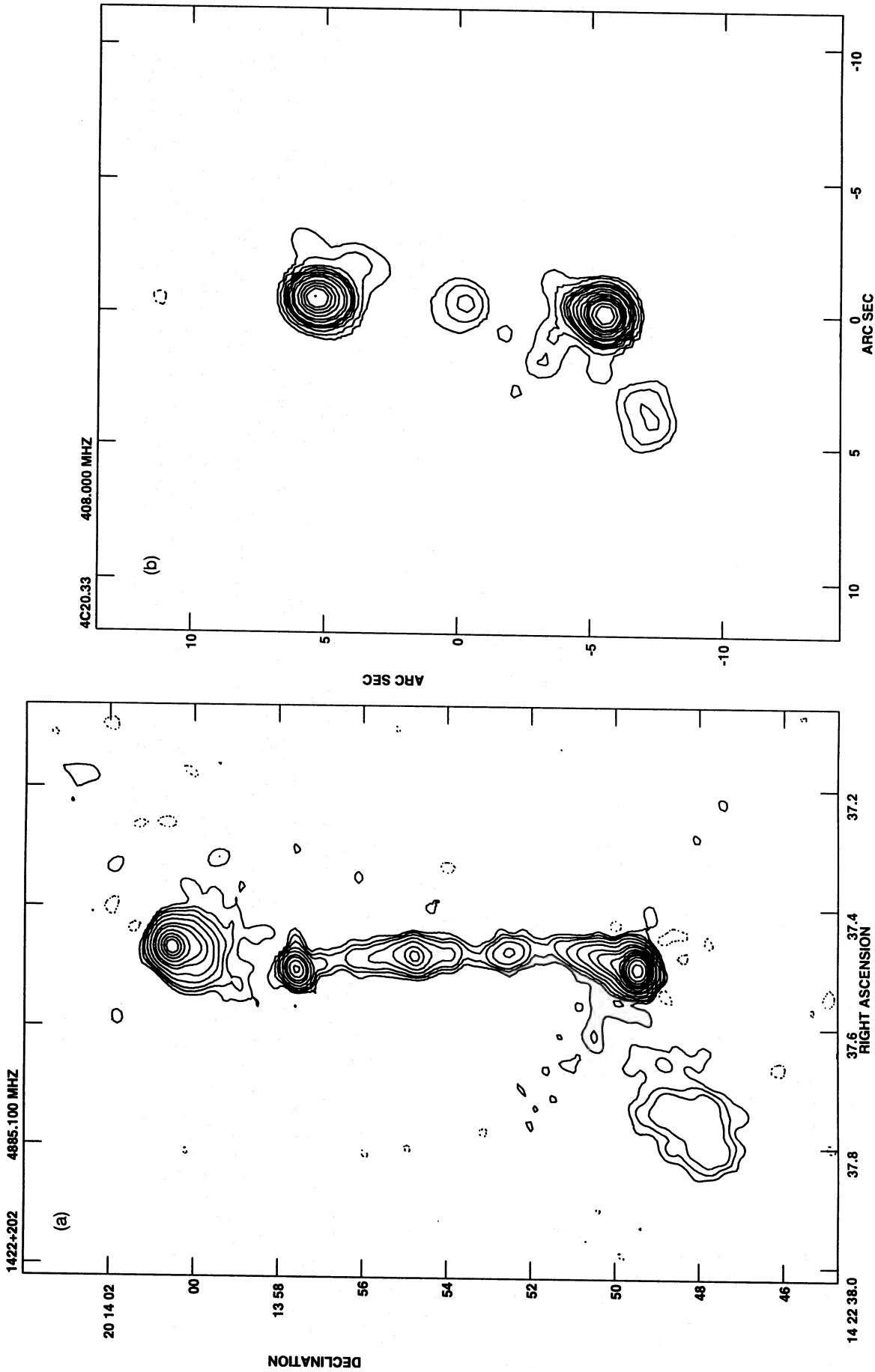


Figure 8. (a) VLA map of 1422+202 at 4885 MHz with an angular resolution of $0.46 \times 0.36 \text{ arcsec}^2$ along a PA of -74° . Peak brightness: $191 \text{ mJy beam}^{-1}$. Contours: $-0.3, 0.3, 0.6, 1, 2, 4, 8, 12, 20, 30, 50, 70, 100, 150$ and $200 \text{ mJy beam}^{-1}$. (b) MERLIN map of 1422+202 at 408 MHz with an angular resolution of $1 \times 1 \text{ arcsec}^2$. Peak brightness: $1314 \text{ mJy beam}^{-1}$. Contours: $-10, 10, 20, 40, 60, 80, 100, 150, 200, 300, 400, 500, 600, 800$ and $1000 \text{ mJy beam}^{-1}$.

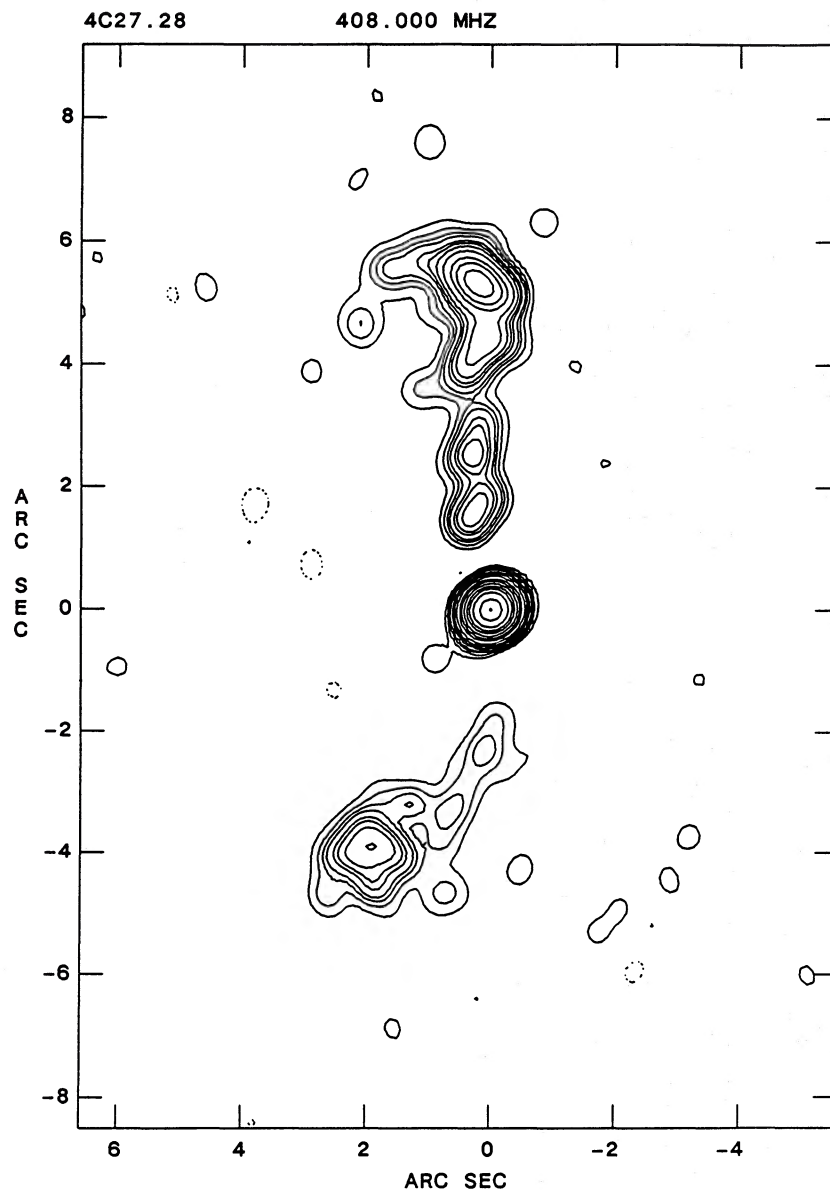


Figure 9. MERLIN map of 1741+279 at 408 MHz with an angular resolution of 0.5×0.5 arcsec². Peak brightness: $713 \text{ mJy beam}^{-1}$. Contours: -2, 2, 4, 6, 8, 12, 15, 20, 30, 50, 70, 100, 150, 200, 300, 500, 700 and $1000 \text{ mJy beam}^{-1}$.

central strong component and two elongated, almost symmetrical features on both sides. The southern jet is weaker and bends towards the east. The northern jet shows several blobs and a ridge of emission with a sickle shape. This source has been identified with a quasar of $m = 17.7$ and $z = 0.372$ (Véron-Cetty & Véron 1987).

2033+187

This source was classified as variable at low frequency by both Cotton (1976) and Fanti *et al.* (1983). Multifrequency observations (Patrielli *et al.* 1987) did not show variability at higher frequencies. The source was observed by Cotton (1983) with the VLA in the A-configuration at three frequencies, 1.4, 5 and 15 GHz, and was found to be unresolved with an angular size < 0.05 arcsec. Our MERLIN map at 408

MHz confirms this compact structure and reveals no extended emission stronger than $\sim 7 \text{ mJy beam}^{-1}$.

2147+145

This source has been classified as variable at low frequency by Cotton (1976) and by Fanti *et al.* (1983). The former observed 2147+145 with the VLA in the A-configuration showing that it is unresolved at 1.4 and 5 GHz and that it appears elongated ($50 \times 30 \text{ mas}^2$ in PA 159°) at 15 GHz (Cotton 1983). Our MERLIN 408-MHz map shows that all the emission comes from an unresolved region. The source was also observed with VLBI at 1.7 GHz by Cotton *et al.* (1984). They found a core-jet structure with an overall size ($< 50 \text{ mas}$) comparable with the Gaussian fit to the 15-GHz VLA observations. On the other hand, more recent VLBI

Table 2. Parameters derived from the VLA observations at 6 cm.

Source name	Other name	rms mJy/b	comp.	Radio Position(B1950)			Flux Density		Major Axis arcsec	PA °
				R.A. h m s	Dec. ° ' "	Peak mJy/b	Total mJy			
0114 – 211		0.4	E	011426.00	-210754.97	61	71			
			W	25.95	55.00	1071	1105			
			Tot				1176			1
0235 – 197		0.05	E	023526.05	-194534.27	76	732			
			W	23.05	30.95	2	98			
			Tot				830			43
0320 + 053	DA101	0.07	C	032041.57	052334.50	715	759	<0.15		
0548 + 165	DA190	0.06	C	054825.20	163556.80	892	938			
			N	25.16	3559.59		24			
			Tot				964	4	-12	
0725 + 147	3C181	0.10	E	072520.49	144344.60	321	439			
			C	.22	46.54	9	9			
			W	.11	47.17	131	227			
			Tot				675			6
0809 – 056		0.08	E	080935.52	-054019.29	177	302			
			W	.19	20.20	76	150			
			Tot				452			5
1203 + 043		0.04	N	120346.87	042301.83	2	50			
			C	.48	2252.48	7	7			
			Jet	.23	47.47	25	102			
			S	45.96	43.91	1	23			
			Tot				194			30
1239 – 044	3C275	0.08	N	123945.09	-042951.46	50	338			
			S	44.82	54.60	293	652			
			Tot				1002			5
1245 – 197		0.10	C	124545.22	-194257.51	2296	2388	<0.15		
1422 + 202	4C20.33	0.08	N	142237.47	201400.46	56	158			
			C	.50	1357.56	34	37			
			Jet	.50	49.48	188	358			
			S				28			
			Tot				581			15
1524 – 136	OR-140	0.08	C	152412.89	-134034.93	924	1184	0.4	26	

327-MHz observations (Cotton, Owen & Mahoney 1989) gave a symmetric and rather extended image of 2147 + 145 that does not resemble the previous 1.7-GHz VLBI structure.

3.2 Observational parameters

Values derived from the VLA A-array, 5-GHz maps are listed in Table 2. The contents of Table 2 are: column 1 – source name; column 2 – other name; column 3 – rms noise in the total intensity map far from the source; column 4 – component labels, North, South, East, West and Core; column 5 – RA and Dec. of the main component peaks; column 6 – peak flux density (mJy); column 7 – total flux density of each source component and of the source as a whole in mJy; column 8 – largest angular size (LAS), defined as the distance from peak to peak for sources with compact outer components or measured to the last reliable contour for diffuse structures (a limit corresponding to one-third of the beam is given

for unresolved sources); column 9 – LAS position angle (PA) in degrees.

Similarly for the MERLIN 408-MHz maps we have in Table 3: column 1 – source name; column 2 – other name; column 3 – rms noise in the total intensity map far from the source; column 4 – the major axis, minor axis in arcsec and the PA in degrees of the restoring beam; column 5 – component labels, North, South, East, West and Core; column 6 – total flux density in mJy of each component and of the source as a whole; column 7 – flux density from compact regions (<one-third of the beam); the values are obtained by modelling the brightness distribution of each component with one or two Gaussians; column 8 – 408-MHz fractional variability in per cent.

In Fig. 10(a) the distribution of the ratio of the VLA 5-GHz flux density to the total power flux density (taken from Kühr *et al.* 1981) is plotted. The median value is 0.96, meaning that our maps generally account for the whole radio emission. The two sources with a ratio of about 0.5

Table 3. Parameters derived from the MERLIN observations at 408 MHz.

Source name	Other name	rms mJy/b	Beam size			comp.	Flux Density		Frac. Var. %
			maj arcsec	min arcsec	PA		Tot mJy	Compact mJy	
0320 + 053	DA101	0.7	0.7	0.6	38	C	6859	6859	14
0548 + 165	DA190	3	0.6	0.5	25	C	4585	4569	
						N	194	-	
						Tot	4779		12
0725 + 147	3C181	3	1.1	0.8	55	E	3331	2326	
						W	4610	2495	
						Tot	7941		9
0809 - 056		2	0.5	0.5		E	3460	1995	
						W	1615	873	
						Tot	5075		8
1239 - 045	3C275	2	0.9	0.7	22	N	2423	957	
						S	7280	4795	
						Tot	9703		6
1422 + 202	4C20.33	2	1.0	1.0		N	1292	615	
						Jet	1830	1480	
						S	114	-	
						Tot	3236		10
1524 - 136	OR-140	2	1.6	1.5	51	C	5465	4950	17
1741 + 279	4C27.28	0.6	0.5	0.5		NJet	480	-	
						C	744	743	
						SJet	157	-	
						Tot	1381		17
2033 + 187		0.9	0.9	0.7	-90	C	2600	2600	21
2147 + 145		17*	5.7	4.8	-22	C	6938	6938	30

*The high rms noise in this map is due to at least five confusing sources which are present in the field of view, namely 2145+151, 2145+150, 2148+143, 2149+140, 2150+146, all having a flux density > 1.5 Jy at 318 MHz (see Douglas *et al.* 1980).

(0235 - 197 and 1203 + 043) are also those that have the largest angular diameters. A similar conclusion can be derived by looking at Fig. 10(b), which plots the ratio between the MERLIN 408-MHz flux density and the total power flux density, taken from Fanti *et al.* (1983). Most of the values are close to 1. The largest discrepancy (~ 0.6) is for the source 1422 + 202, which shows extended structure also. It is possible that some low-brightness emission has been resolved out by the MERLIN array. For this source the percentage of 408-MHz variability reported in Table 3 is normalized to the MERLIN total flux density.

3.3 Comments on sources from literature

For five sources in our sample, arcsecond and milliarcsecond observations can be found in the literature. Information on their structures can be summarized as follows.

0358 + 004 (3C99)

This source is discussed extensively by Mantovani *et al.* (1990b). The arcsecond-scale observations show that 3C99

is a double-lobed source with a moderately strong core. The outer components are located very asymmetrically relative to the nucleus and have rather different surface brightnesses. The source was found to be variable at 408 MHz by Fanti *et al.* (1983) and not variable at higher frequencies (Padielli *et al.* 1987).

0518 + 165 (3C138)

This source, classified as a low-frequency variable by Fanti *et al.* (1983), shows a core-jet structure at the arcsecond scale (van Bruegel 1984). It was exhaustively observed with VLBI by Fanti *et al.* (1989) and is considered to be a prototype CSS source.

0621 + 410 (3C159)

This is an extended double radio source identified with a 19-mag emission-line galaxy at $z=0.482$ (Tytler & Browne 1985). Browne *et al.* (1985) suggested that the variations at 408 MHz (Fanti *et al.* 1981) could arise from the combined effect of high linear polarization and changes in ionospheric Faraday rotation.

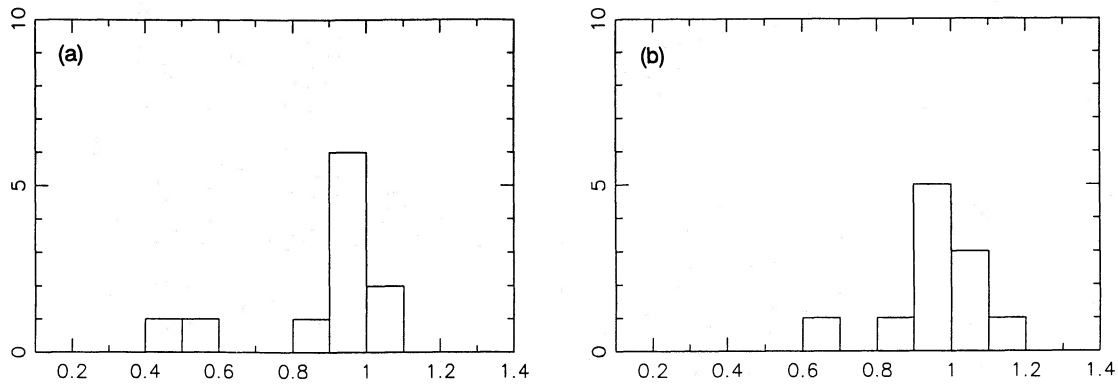


Figure 10. (a) Distribution of the ratio of the VLA 5-GHz flux density to the total power flux density. (b) Distribution of the ratio of the MERLIN 408-MHz flux density to the total power flux density.

1117+114

This source was found to be variable at low frequency by Fanti *et al.* (1983) and by Altschuler *et al.* (1984). It is a point source with the VLA at a resolution of ~ 0.4 arcsec (Perley 1982). The source has a VLBI correlated flux density < 60 mJy at 2.29 GHz (Preston *et al.* 1985). A recent VLBI map made with a global array at 610 MHz (Patrielli *et al.* 1991) shows two symmetric, slightly resolved components separated by 69 mas in PA 80° , which account for the whole total power flux density. The optical counterpart is a quasar with $m = 20$.

1358+628

This source, which shows variability only in the low-frequency band (Fanti *et al.* 1983; Patrielli *et al.* 1987), was not resolved by Perley (1982) using the VLA at 20 and 6 cm. Preston *et al.* (1985) measured a correlated flux density of 220 mJy with a VLBI observation at 2.29 GHz. The source was also observed at 610 MHz with a global array by Patrielli *et al.* (1991). The structure is a symmetric double with the two components separated by ~ 40 mas in PA 125° , embedded in a halo. The VLBI map accounts for the whole total power flux density. 1358+628 has been identified with a galaxy of redshift 0.429 (Lawrence *et al.* 1986).

4 CONCLUSIONS

Table 4 summarizes the available optical information on the whole sample of sources, along with linear sizes. It contains optical coordinates, optical identification, visual magnitude, redshift and linear size in kpc (computed for $q_0 = 1$ and $H_0 = 100 \text{ km s}^{-1} \text{ Mpc}^{-1}$, $z = 1$ was assumed for sources with redshift not available). References are also added to the table.

Some broad conclusions can be drawn from Table 4. About half of the sources appear to be unresolved or only marginally resolved by arcsecond-resolution observations. Therefore the selection criterion we have adopted, i.e. variability at 408 MHz, has allowed us to select steep-spectrum sources which are compact on arcsecond scales.

The distribution of the largest linear sizes is shown in Fig. 11. All but three of the 19 sources are smaller than 43 kpc

(median value 10 kpc). Steep-spectrum sources with such linear sizes are usually considered members of the CSS class (see for example Fanti *et al.* 1990).

A classification based on the arcsecond-scale structure of the sources, and from the information available in the literature, allows us to separate them into sources dominated by an unresolved steep-spectrum component and lobe-dominated sources (denoted as c and l respectively in Table 4, column 8). The two groups are shown below.

Dominated by an unresolved component	Lobe-dominated
0114-211	0235-197
0320+053	0621+410
0358+004	0725+147
0518+165	0809-056
0548+165	1203+043
1117+114	1239-045
1245-197	1422+202
1358+628	
1524-136	
1741+279	
2033+187	
2147+145	

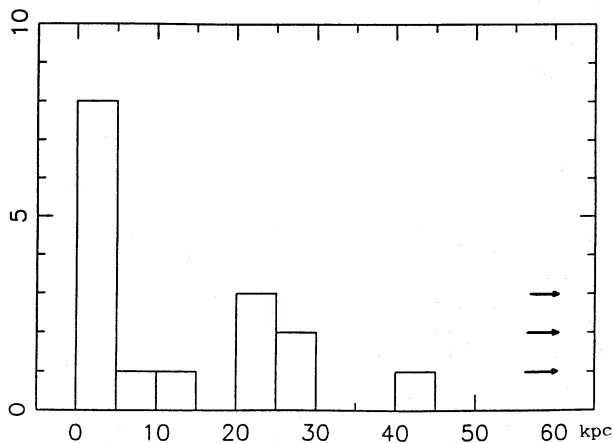
The sources in the first group are classified as CSS sources and clearly show the existence of compact (arcsecond) components, as required from their variability. Most of their 408-MHz flux density originates in components with angular sizes $\lesssim 300$ mas. These components are bright enough to account for the fractional variability we reported in column 8 of Table 3.

More than half of the lobe-dominated sources can also be classified as CSS sources. In three cases, however, 0235-197, 0621+410 (3C159) and 1203+043, the VLA 5-GHz maps show compact components which are too weak to account for the observed variability. In these cases it is possible that the variability is spurious, or caused by instrumental effects. For instance, Browne *et al.* (1985) and Cerchiara *et al.* (in preparation) suggest that ionospheric Faraday rotation is the cause of the variability of 3C159, which is significantly polarized at 408 MHz. It would be of interest to check if 0235-197 and 1203+043 are highly polarized too.

Table 4. Optical information and linear sizes.

Source name	Other name	Optical Position		Opt. Id.	m	z	L.S. kpc	Cl.	Ref
		R.A.(B1950)	Dec.(B1950)						
0114 - 211				G	19		7	c	
0235 - 197		02 35 24.77	-19 45 31.77	G	21.3	0.62	160	l	a
0320 + 053	DA101	03 20 41.25	05 23 34.3	G	20.9		<2	c	b
0358 + 004	3C99	03 58 33.28	00 28 10.6	G	20.2	0.426	21	c	c
0518 + 165	3C138	05 18 16.5	16 35 27	Q	17.9	0.759	3	c	d
0548 + 165	DA190	05 48 25.22	16 35 56.4	BSO	17		14	c	e
0621 + 410	3C159	06 21 33.77	40 05 30.0	G	19	0.482	110	l	f
0725 + 147	3C181	07 25 20.28	14 43 46.7	Q	18.9	1.382	25	l	e
0809 - 056							24	l	
1117 + 628				Q			<2	c	g
1203 + 043							120	l	
1239 - 044	3C275	12 39 45.16	-04 29 53.9	G	21	0.48	22	l	
1245 - 197		12 45 45.24	-19 42 58.2	Q		1.275	<2	c	h
1358 + 628	4C62.22			G	19.8	0.429	<2	c	i
1422 + 202	4C20.33	14 22 37.488	20 13 57.54	Q	17.6	0.871	43	l	l
1524 - 136	OR-140	15 24 12.84	-13 40 31.1	Q	20.5	1.687	3	c	m
1741 + 279	4C27.28	17 41 57.9	27 54 04	Q	17.7	0.372	29	c	n
2033 + 187							<2	c	
2147 + 145		21 47 59.35	14 35 45.7		20.7		<2	c	o

G - galaxy; Q - quasar; BSO - blue stellar object. References: a - position from Prestage & Peacock (1983); z from Morganti (private communication); b - position from Broderick & Condon (1975); c - Spinrad *et al.* (1985); d - Véron-Cetty & Véron (1989); e - Wills *et al.* (1973); f - Tytler & Browne (1985); g - Preston *et al.* (1985); h - position from Walter & West (1980); z from Morganti (private communication); i - Lawrence *et al.* (1986); l - Argue *et al.* (1973); m - position from Véron *et al.* (1976); z from Hunstead (private communication); n - Schmidt (1974); o - position from Cotton *et al.* (1989).

**Figure 11.** Distribution of the linear sizes in kpc.

The four other lobe-dominated CSS sources are the most interesting from the point of view of the LFV phenomenon. They show regions of more diffuse emission in which compact hotspots (angular sizes ≤ 300 mas) are embedded (see Table 3). The hotspots are bright enough to account for the fractional variability, which is on the average lower than that of the core-dominated sources.

Although VLBI observations are needed to confirm the presence of the compact structures, our results indicate that LFV occurs in sources with compact regions far from the active core. Since the cores are too weak to give rise to the observed variability, this observation strongly suggests that the LFV of this class of sources is due to extrinsic mechanisms. Bååth & Mantovani (1991) had hypothesized earlier that the variability of 1422 + 202 was connected with the southern hotspot.

ACKNOWLEDGMENTS

We thank R. Morganti and R. W. Hunstead who provided redshifts prior to publication. FM thanks the Director, Jodrell Bank and the Director, NRAO, Socorro, for their hospitality during periods when parts of the work were done. Associated Universities Incorporated operates the National Radio Astronomy Observatory under National Science Foundation Cooperative Agreement No. AST8814515.

REFERENCES

Altshuler, D. R., Broderick, J. J., Condon, J. J., Dennison, B., Mitchell, K. J., O'Dell, S. L. & Payne, H. E., 1984. *Astr. J.*, **89**, 1784.

- Argue, A. N., Kenworthy, C. M. & Stewart, P. M., 1973. *Astrophys. Lett.*, **14**, 99.
- Bååth, L. B. & Mantovani, F., 1991. *Radio Interferometry Theory, Techniques and Applications*, Astr. Soc. Pacif. Conf. Series No. 19, p. 298, eds Cornwell, T. J. & Perley, R. A., Astr. Soc. Pacif., San Francisco.
- Blandford, R. D. & Königl, A., 1979. *Astrophys. J.*, **232**, 34.
- Broderick, J. J. & Condon, J. J., 1985. *Astrophys. J.*, **202**, 596.
- Browne, I. A. W., Mantovani, F., Muxlow, T. W. B., Padrielli, L. & Romney, J., 1985. *Mon. Not. R. astr. Soc.*, **213**, 945.
- Burbidge, G. R., Jones, T. W. & O'Dell, S. L., 1974. *Astrophys. J.*, **193**, 43.
- Cawthorne, T. W., Scheuer, P. A. G., Morison, I. & Muxlow, T. W. B., 1986. *Mon. Not. R. astr. Soc.*, **219**, 883.
- Cotton, W. D., 1976. *Astrophys. J. Lett.*, **204**, L63.
- Cotton, W. D., 1983. *Astrophys. J.*, **271**, 51.
- Cotton, W. D., Owen, F. N. & Mahoney, M. J., 1989. *Astrophys. J.*, **338**, 37.
- Cotton, W. D., Owen, F. N., Geldzahler, B. J., Johnston, K., Bååth, L. & Romney, J., 1984. *Astrophys. J. Lett.*, **277**, L41.
- Davis, R. J., Stannard, D. & Conway, R. G., 1983. *Mon. Not. R. astr. Soc.*, **205**, 1267.
- Dennison, B., Broderick, J. J., O'Dell, S. L., Mitchell, K. J., Altschuler, D. R., Payne, H. E. & Condon, J. J., 1984. *Astrophys. J. Lett.*, **281**, L55.
- Douglas, J. N., Bash, F. N., Torrence, G. W. & Wolfe, C., 1980. *The University of Texas Publications in Astronomy* No. 17, Austin, Texas.
- Fanti, C., Fanti, R., Ficarra, A., Mantovani, F., Padrielli, L. & Weiler, K. W., 1981. *Astr. Astrophys. Suppl.*, **45**, 61.
- Fanti, C., Fanti, R., Ficarra, A., Gregorini, L., Mantovani, F. & Padrielli, L., 1983. *Astr. Astrophys.*, **118**, 171.
- Fanti, R., Fanti, C., Schilizzi, R. T., Spencer, R. E., Nan Rendong, Parma, P., van Breugel, W. J. M. & Venturi, T., 1990. *Astr. Astrophys.*, **231**, 333.
- Fanti, C., Fanti, R., Parma, P., Venturi, T., Schilizzi, R. T., Nan Rendong, Spencer, R. E., Muxlow, T. W. B. & van Breugel, W. J. M., 1989. *Astr. Astrophys.*, **217**, 44.
- Giacani, E. B. & Colomb, F. R., 1988. *Astr. Astrophys. Suppl.*, **76**, 15.
- Gregorini, L., Ficarra, A. & Padrielli, L., 1986. *Astr. Astrophys.*, **168**, 25.
- Jones, T. W. & Burbidge, G. R., 1973. *Astrophys. J.*, **186**, 791.
- Kühr, H., Nauber, U., Pauliny-Toth, I. I. K. & Witzel, A., 1981. Max-Planck-Institut für Radioastronomie, preprint No. 55.
- Lawrence, C. R., Pearson, T. J., Readhead, A. C. S. & Unwin, S. C., 1986. *Astr. J.*, **91**, 494.
- Mantovani, F., Muxlow, T. W. B. & Padrielli, L., 1987. *The Impact of VLBI on Astrophysics and Geophysics*, IAU Symp. No. 129, p. 125, eds Reid, M. J. & Moran, J. M., Kluwer, Dordrecht.
- Mantovani, F., Fanti, R., Gregorini, L., Padrielli, L. & Spangler, S. R., 1990a. *Astr. Astrophys.*, **233**, 535.
- Mantovani, F., Saikia, D. J., Browne, I. W. A., Fanti, R., Muxlow, T. W. B. & Padrielli, L., 1990b. *Mon. Not. R. astr. Soc.*, **245**, 427.
- McAdam, W. B., 1980. *Proc. astr. Soc. Aust.*, **4**, 70.
- Padrielli, L., Eastman, W., Gregorini, L., Mantovani, F. & Spangler, S. R., 1991. *Astr. Astrophys.*, **249**, 351.
- Padrielli, L., Aller, M. F., Aller, H. D., Fanti, C., Fanti, R., Ficarra, A., Gregorini, L., Mantovani, F. & Nicolson, G., 1987. *Astr. Astrophys. Suppl.*, **67**, 63.
- Perley, R. A., 1982. *Astr. J.*, **87**, 859.
- Prestage, R. M. & Peacock, J. A., 1983. *Mon. Not. R. astr. Soc.*, **204**, 355.
- Preston, R. A., Morabito, D. D., Williams, J. G., Faulkner, J., Jauncey, D. L. & Nicolson, G. D., 1985. *Astr. J.*, **90**, 1599.
- Rees, M. J., 1966. *Nature*, **211**, 468.
- Rickett, B. J., 1986. *Astrophys. J.*, **307**, 564.
- Rickett, B. J., Coles, W. A. & Bourgeois, G., 1984. *Astr. Astrophys.*, **134**, 390.
- Saikia, D. J., 1988. In: *Active Galactic Nuclei*, p. 327, eds Miller, H. R. & Wiita, P. J., Springer-Verlag, Berlin.
- Schmidt, M., 1974. *Astrophys. J.*, **193**, 505.
- Shapirovskaia, N. Ya., 1982. *Soviet Astr.*, **26**, 151.
- Spangler, S. R. & Cotton, W. D., 1981. *Astr. J.*, **86**, 730.
- Spangler, S. R., Fanti, R., Gregorini, L. & Padrielli, L., 1989. *Astr. Astrophys.*, **209**, 315.
- Spencer, R. E., McDowell, J. C., Charlesworth, M., Fanti, C., Parma, P. & Peacock, J. A., 1989. *Mon. Not. R. astr. Soc.*, **240**, 657.
- Spinrad, H., Kron, R. G. & Hunstead, R. W., 1979. *Astrophys. J. Suppl.*, **41**, 701.
- Spinrad, H., Djorgovski, S., Marr, J. & Aguilar, L., 1985. *Publs astr. Soc. Pacif.*, **97**, 932.
- Thomasson, P., 1986. *Q. J. R. astr. Soc.*, **27**, 413.
- Thompson, A. R., Clark, B. G., Wade, C. M. & Napier, P. J., 1980. *Astrophys. J. Suppl.*, **44**, 151.
- Tytler, D. & Browne, I., 1985. *Astr. J.*, **90**, 1676.
- van Breugel, W. J. M., Miley, G. K. & Heckman, T. M., 1984. *Astr. J.*, **89**, 5.
- Véron-Cetty, M. P. & Véron, P., 1989. *ESO Scientific Report No. 7*, Garching.
- Véron, M. P., Véron, P., Adgie, R. L. & Gent, H., 1976. *Astr. Astrophys.*, **47**, 401.
- Walter, H. G. & West, R. M., 1980. *Astr. Astrophys.*, **86**, 1.
- Wills, B. J., Wills, D. & Douglas, J. N., 1973. *Astr. J.*, **78**, 521.